

Blood Vessels Segmentation in Retina: Preliminary Assessment of the Mathematical Morphology and of the Wavelet Transform Techniques

JORGE J. G. LEANDRO¹
ROBERTO M CESAR JR¹
HERBERT F. JELINEK²

¹Department of Computer Science – IME - USP, Rua do Matão, 1010, São Paulo, SP, 05508-900 Brazil

²School of Community Health, Charles Sturt University, Albury 2640, Australia

e-mails: ¹{jleandro,cesar}@ime.usp.br ²hjelinek@csu.edu.au

<http://www.ime.usp.br/~cesar/>

Abstract: This work reports the development of a system for automatic analysis of retinal angiographic images. Particularly, we focus on the segmentation of the blood vessels in these images. We started by implementing a previously known technique based on mathematical morphology. Due to some shortcomings of this method to our data, we have developed a new approach based on the continuous wavelet transform using the Morlet wavelet. The main advantage of the latter with respect to our images lies in its capabilities in tuning to specific frequencies, thus allowing noise filtering and blood vessel enhancement in a single step. Furthermore, as we intend to use shape analysis techniques for the detection and quantitative characterisation of the vascular branching pattern in the retina, the wavelets will also be important with respect to performing fractal and multifractal image analysis. Nevertheless, it is worth mentioning that the mathematical morphology method was able to detect finer detail more precisely. Our present results suggest that an interesting direction to be investigated is how to use both approaches together in order to obtain better results and apply this as a diagnostic tool.

Keywords: biological shape analysis; multiscale methods; mathematical morphology; wavelets; retina; pathology.

1 Introduction

Proliferative diabetic retinopathy (PDR) is characterised by new vessel growth near or at the optic disk (blind spot) or elsewhere in the peripheral retina and is known as a risk factor for severe vision loss [Sussman et al., 1982]. However, the effectiveness of the treatment depends on the timely detection of these vascular changes. Additional fundal pathology, such as cataracts, often minimize a timely detection of vascular changes and may lead to uncertain diagnosis. Advances in shape analysis, and the development of strategies for the detection and quantitative characterisation of proliferative vascular changes is therefore of great importance.

Fluorescein angiograms highlight the blood vessel network of the retina and allows one to evaluate the progression of vascular disease. Recently we have developed a semi-automated process for image processing and shape analysis [Cesar & Costa, 1999]. The new method, which is based on multiscale curvature contour segmentation and syntactic shape analysis, is robust and greatly improves the tiresome task of drawing branching

structures such as the vessel networks prior to analysis (see Mainster, 1990; Daxer, 1993). A necessary initial step in applying shape analysis is to segment the blood vessels from the background. This work describes the results we obtained with an algorithm to segment only the vascular tree of retinal angiograms by applying mathematical morphology operations [Walter *et al.*, 2000]. Mathematical morphology has previously revealed itself as a very useful digital image processing technique for quantifying retinal pathology by detecting and counting micro-aneurysms in fluorescein angiograms [Spencer *et al.*, 1996]. Furthermore, we describe a new approach based on the continuous wavelet transform (CWT), and compare the results obtained with this approach to that of mathematical morphology. The continuous wavelet transform (CWT) is a powerful and versatile tool that has been applied in many different image processing problems, from image coding [Rioul & Vetterli, 1991] to shape analysis [Costa & Cesar, 2001]. This success is largely due to the fact that wavelets are

especially suitable for detecting singularities (e.g. edges) in signals [Grossmann, 1988], extracting instantaneous frequencies [Antoine & Murenzi, 1994], and performing fractal and multifractal analysis [Jones and Jelinek, 2001; Arnéodo *et al.*, 2000]. Furthermore, the wavelet transform using the Morlet wavelet, also often referred to as *Gabor wavelet*, has played a central role in increasing our understanding of visual processing in different contexts from feature detection to face tracking. The next section of this paper describes our implementation of the previously proposed mathematical morphology approach to the segmentation problem. In what follows, Section 3 describes our new approach based on Morlet wavelets. Some illustrative experimental results are presented and discussed in Section 4. Finally, Section 5 concludes with some comments on our ongoing work.

2 Mathematical Morphology Approach

The notation and definitions in this section follow those adopted by Gonzalez and Woods [1992] and Banon and Barrera [1994]. In this section we describe our implementation of mathematical morphology proposed in [Walter *et al.*, 2000].

Let $(x,y) \in \mathbb{Z} \times \mathbb{Z}$, \mathbb{Z} denote the set of integer numbers, and $f, b \in \mathbb{Z}^2$ be two discrete functions representing the digital image and the structuring element respectively, that assign a certain gray level value, here an integer number g , $255 \geq g \geq 0$, to each distinct pair of coordinates (x,y) .

Basically, most of the mathematical morphology operations lie on erosions and dilations, whose formal definitions may be respectively written according equations (1) and (2):

$$\mathcal{E}(f,b)(s,t) = \min \{ f(s+x, t+y) - b(x,y) \mid (s+x, t+y) \in D_f, (x,y) \in D_b \} \quad (1)$$

$$\mathcal{D}(f,b)(s,t) = \max \{ f(s-x, t-y) + b(x,y) \mid (s-x, t-y) \in D_f, (x,y) \in D_b \} \quad (2)$$

D_f and D_b are the domains of the functions f and b respectively.

As our main aim was to segment the vascular tree present in the retinal image, we had to initially remove all the non-linear abrupt gray level variations, say the aneurysms [Walter *et al.*, 2000]. To do so, we took the supremum of the openings with elongated 10 pixel-sized structuring elements whose length was larger than the diameter of an aneurysm in different rotational directions. These orientations were taken within rates of 10 degrees from 0 up to a maximum of 180 degrees. Following this strategy, we were able to preserve elongated structures

that corresponded with the vascular tree we intended to segment.

The Opening operation is defined as an erosion followed by a dilation with a specific structuring element being mathematically represented as:

$$\gamma(f,b) = \mathcal{D}(\mathcal{E}(f,b), b) \quad (3)$$

where b is the proper structuring element and f the digital function to be opened.

The above procedure allowed us to smooth vessels, to break the narrow items and to eliminate the thin protrusions. Figure 1 is a representation of an angiographic image that we have used for the experiments in this work, while Figure 2 illustrates the result of the aforementioned supremum of openings procedure.

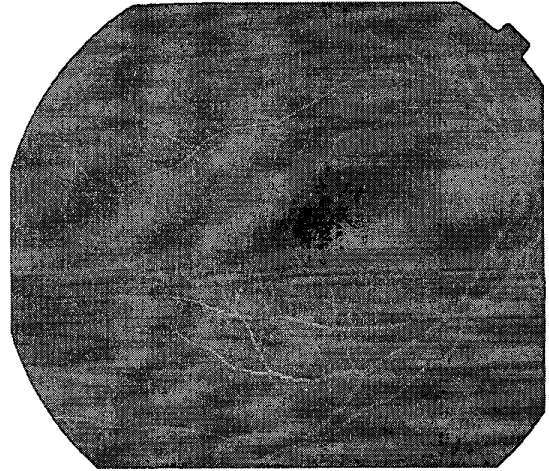


Figure 1: Original angiographic image of the retina.

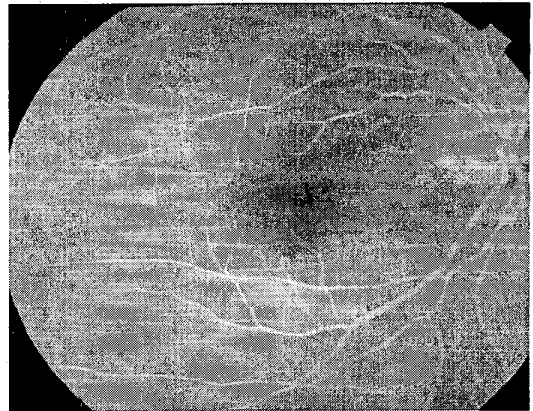


Figure 2 The result obtained by supremum of openings

Then we computed the sum of top-hats by using linear 10 pixel-sized structuring elements rotated in increments of 10 degrees up to a maximum of 180 degrees. The main feature of the top-hat transform is to emphasize detail (smaller vessels) in the presence of shadow (the background).

The top-hat transform may be mathematically defined according to the equation (4):

$$\text{tophat}(f,b)=f-\hat{\delta}(f,b) \quad (4)$$

where b is the proper structuring element and f the digital function to be transformed

Figure 3 shows the result from this latter step.

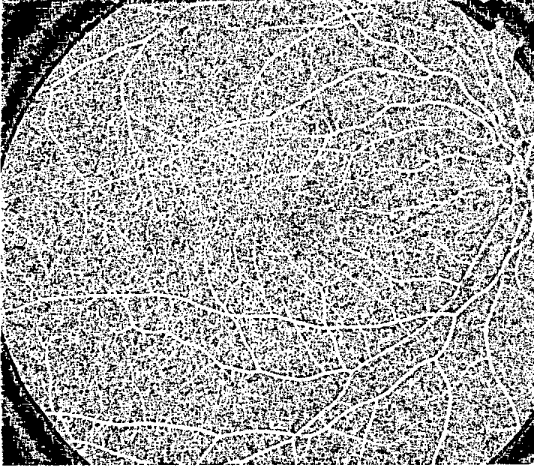


Figure 3: The result obtained by the Top-Hat Transform application

Thirdly, we followed two methods for edge detection: the Canny and the LoG filters. The latter provided the best results (see Figure 4). The LoG (Laplacian of Gaussian) is based on differential operators and may be defined in polar coordinates, since the circular symmetry holds, as:

$$\text{LoG}(r)=\left(\frac{r^2-2\sigma^2}{2\pi\sigma^6}\right)e^{-\left(r^2/2\sigma^2\right)} \quad (5)$$

Finally, to preserve the edges whilst reducing spurious noise, we used alternating sequential filtering (ASF). ASF increased the length of the structuring elements, from 10 up to 30 pixels and in rotational orientations at 30 degree increments up to 180 degrees. This step was applied to eliminate the structures

associated with noise. The final result is presented and discussed in Section 4.



Figure 4: The result obtained by the LoG filtering

3 Wavelet Transform Approach

The notation and definitions in this section follows Arnéodo et al, [2000]. The real plane $R \times R$ is denoted as R^2 , and the vectors are represented as bold letters, e.g. $\mathbf{x}, \mathbf{b} \in R^2$. Let $f \in L^2$ be an image represented as a square integrable (i.e. finite energy) function defined over R^2 . The *continuous wavelet transform (CWT)* $T_\psi(\mathbf{b}, \theta, a)(\mathbf{x})$ is defined as:

$$T_\psi(\mathbf{b}, \theta, a)(\mathbf{x}) = C_\psi^{-1/2} \frac{1}{a} \int \psi^*(a^{-1}r_{-\theta}(\mathbf{x} - \mathbf{b}))f(\mathbf{x})d^2\mathbf{x} \quad (6)$$

In the above formula (6), C_ψ , ψ , \mathbf{b} , θ and a denote the normalizing constant, analyzing wavelet, the displacement vector, the rotation angle and the dilation parameter (ψ^* denotes the complex conjugate). As previously mentioned, the CWT is a useful tool for detecting and analyzing singularities, such as edges in images. There are many different analyzing wavelets that can be adopted, such as the 2D Mexican hat, the optical wavelet and the Morlet wavelet. In this work, we have chosen the Morlet wavelet because it is directional (in the sense of being effective in selecting orientations) and capable of fine tuning specific frequencies. This latter capability is especially important in filtering out the background noise of the angiographic images. These characteristics of the Morlet wavelet represent its

advantages with respect to other standard filters such as the Gaussian and its derivatives. The 2D Morlet wavelet is defined as:

$$\psi_M(\mathbf{x}) = \exp(j \mathbf{k}_0 \cdot \mathbf{x}) \exp\left(-\frac{1}{2} |A\mathbf{x}|^2\right) \quad (7)$$

where $j = \sqrt{-1}$ and $A = \text{diag}[\varepsilon^{-1/2}, 1]$, $\varepsilon \geq 1$ is a 2×2 array that defines the anisotropy of the filter, i.e. its elongation in some direction [Antoine & Murenzi, 1994]. In the Morlet equation (7), which is actually a complex exponential multiplying a 2D Gaussian, \mathbf{k}_0 is a vector that defines the frequency of the complex exponential. Figure 5 illustrates the Morlet wavelets for different sets of parameters.

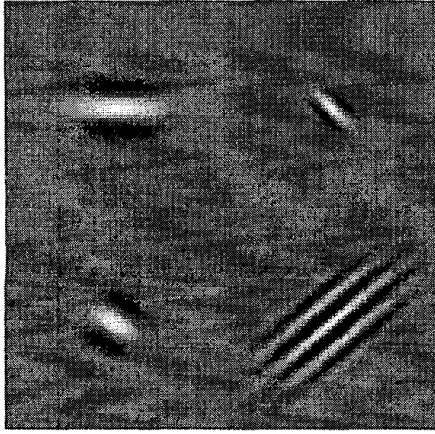


Figure 5: Morlet wavelets (real part) for 4 different set of parameters, showing its capabilities for tuning to scale, orientation, position and frequency.

Using the Morlet transform to segment the blood vessels, the scale parameter is held constant and the transform is calculated for a set of orientations $\theta = 0, 10, 20, 30, \dots, 180$. The ε parameter has been set as 4 in order to make the filter elongated and $\mathbf{k}_0 = [0 \ 2]$, i.e. a low frequency complex exponential with few significant oscillations. These two characteristics have been chosen in order to enable the transform to present stronger responses for the coefficients associated with the blood vessels. Figure 6 shows the wavelet transform of the angiographic image of Figure 1 for two different orientations θ . The transform maximum response (in modulus) from all orientations for each position, \mathbf{b} , is then taken (Figure 7), emphasizing the blood vessels and filtering out most of the noise and other undesirable features. The blood

vessels can then be detected from this representation. We have tried three different image segmentation approaches to segment the blood vessel network following the Morlet transform application: adaptive thresholding, edge detection and semi-interactive region-growing. The basic algorithm can be stated as follows:

Algorithm for Blood Vessels Segmentation

```

Set  $T_{\max}(\mathbf{b}) = 0, \forall \mathbf{b}$ 
for each  $\theta = 0, 10, 20, 30, \dots, 180$ 
  Calculate  $|T_{\psi}(\mathbf{b}, \theta, a)(\mathbf{x})|$ 
  Set  $|T_{\psi}(\mathbf{b}, \theta, a)(\mathbf{x})| = 0$  if  $|T_{\psi}(\mathbf{b}, \theta, a)(\mathbf{x})| < t_n \ \forall \mathbf{b}$ 
  Set  $T_{\max}(\mathbf{b}) = \max(T_{\max}(\mathbf{b}), |T_{\psi}(\mathbf{b}, \theta, a)(\mathbf{x})|) \ \forall \mathbf{b}$ 
end_for

Find the blood vessels from  $T_{\max}(\mathbf{b})$ 

```

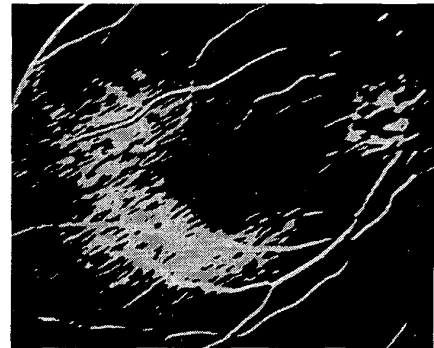


Figure 6: Wavelet transform response for two different orientations.

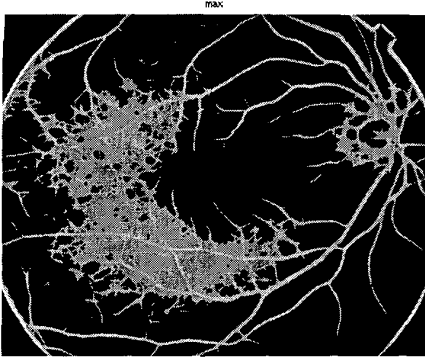


Figure 7: Wavelet transform taking the maximum response for all orientations $\theta = 0, 10, 20, 30 \dots 180$.

In the above algorithm, t_n is a threshold and the step involving it (second step within the **for**) is carried out in order to set the noise coefficients with weak response to 0. This operation is commonly referred to as *shrinkage* by the wavelets community.

The last step required for segmenting and enhancing the blood vessels has been implemented by using three different strategies, as previously mentioned. The adaptive thresholding technique has been adapted from [Ficher et al, 1996]. Adaptive thresholding is obtained by comparing the value of each position b with $\mu - c$, where μ is the mean value around b and c is a constant introduced to avoid noisy segmentation along uniform background regions. The size of the neighborhood where the mean value is calculated is an input parameter, and we have used a small 5×5 window. Wavelet coefficients larger than $\mu - c$ are associated to blood vessels, while those smaller are considered background. For the edge detection experiments, we have simply applied the Sobel approach [Gonzalez & Woods, 1992]. Finally, we have also tried a traditional semi-interactive region-growing algorithm [Gonzalez & Woods, 1992], as discussed in the next section.

4 Experimental Results

The series of intermediary results obtained by the mathematical morphology approach has lead to the segmented image shown in Figure 8. As can be seen, the blood vessels have been segmented, including some difficult fine structures, though some noise has remained.

On the other hand, the Morlet wavelets approach, whose maximum response for the considered orientations is shown in Figure 7, has lead to the segmented results of Figures 9, 10 and 11, produced by segmentation using adaptive thresholding, Sobel edge detection and region-growing, respectively. The region growing approach has been applied with a set of seeds indicated interactively by the user. Clearly, the main problem of the wavelets approach is the grey central region, which produces some noisy structures for the automatic segmentation methods (adaptive thresholding and Sobel). This problem has been circumvented by the region-growing approach, but at the expense of a semi-interactive technique. We have applied the Morlet wavelets technique to other different images and obtained similar results.



Figure 8: The final result obtained by the mathematical morphology approach.

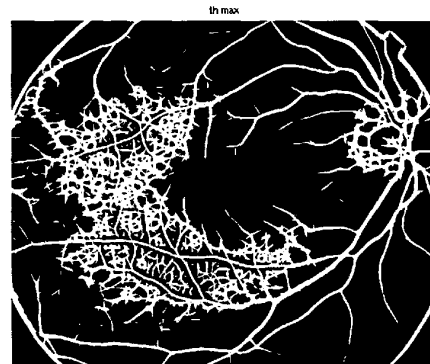


Figure 9: Segmented image using adaptive thresholding.

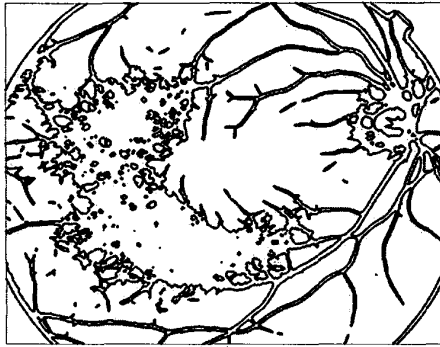


Figure 10: Result of edge detection from the wavelet transform of Figure 9

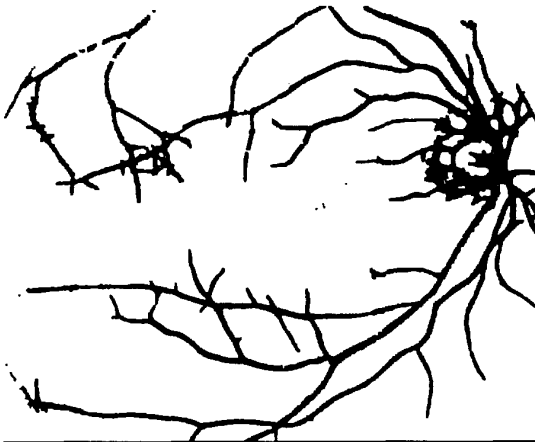


Figure 11: Segmented blood vessels using semi-interactive region-growing.

It is worth mentioning that extensive experiments with the Morlet wavelets approach has been carried out for different sets of parameters, which can be found at:

<http://www.vision.ime.usp.br/~cesar/projects/sibgrapi2001/>

It is clear that many sets of parameters lead to similar (good) results, suggesting that correct parameter setting is not so critical. On the other hand, some sets of parameters with high frequency modulating exponentials produce very noisy results, indicating that proper care should be taken.

5 Concluding Remarks

Our results indicated that retinal vessels can be segmented in the fundus of the eye with some noise by

using either mathematical morphology or wavelet transforms. The main advantage of the wavelet approach lies in its capabilities in tuning on specific frequencies. This allows noise filtering and blood vessel enhancement in a single step. The good local contrast exhibited by the blood vessels suggested that using more powerful segmentation algorithms, such as those based on gradient and morphological reconstruction [Fisher *et al*, 1996], should lead to better vessels segmentation results. This will be incorporated soon in our system. Furthermore, the wavelet transform can also be used to perform fractal and multifractal analysis, which is a powerful shape analysis tool *per se*. On the other hand, the mathematical morphology method was able to detect finer detail more precisely in our experiments. Therefore, both methods have demonstrated that automated processing of the retinal fundus can select the retinal vasculature, which then allows further automated processing to determine the spatial characteristics of the vascular network and serve as a diagnostic tool in retinal disease. Our ongoing work aims at obtaining more precise results by mixing the results from both approaches discussed in this paper. Finally, we have also started the second phase of the project regarding shape analysis of the blood vessels in order to quantitatively characterize vascular changes associated with diabetic retinopathy such as neovascularisation and microaneurysms.

Acknowledgements

Roberto M. Cesar Jr. is grateful to FAPESP (99/12765-2) and to CNPq (300722/98-2 and 468413/00-6).

References

- J-P. Antoine & R. Murenzi, Two-Dimensional Wavelet Analysis in Image Processing, *Physica Magazine*, 16:105-134, 1994.
- A. Arnéodo, N. Decoster and S.G. Roux, A wavelet-based method for multifractal image analysis. I. Methodology and test applications on isotropic and anisotropic random rough surfaces, *The European Physical Journal B*, 15: 567-600, 2000.
- G.J.F. Banon & J. Barrera, *Bases da Morfologia Matemática para Análise de Imagens Binárias*, Escola de Computação (Recife - PE), 1994.
- R.M. Cesar Jr. and L. da F. Costa, Dendrogram generation for neural shape analysis, *The Journal of Neuroscience Methods*, 93:121-131, 1999.
- L.F.Costa & R.M.Cesar Jr, *Shape Analysis and Classification: Theory and Practice*, CRC Press, 2001.
- A. Daxer, The fractal geometry of proliferative diabetic retinopathy: implications for the diagnosis and the process of retinal vasculogenesis, *Current Eye Research*, 12(12):1103-1109, 1993.

R. Fisher, S. Perkins, A. Walker and E. Wolfart, *HIPR - The Hypermedia Image Processing Reference*, J. Wiley & Sons, 1996.

R.F. Gonzalez & P. Woods, *Digital Image Processing*, Addison-Wesley, 1992

A. Grossmann, Wavelet Transforms and Edge Detection, in S. Albeverio, Ph. Blanchard, M. Hazewinkel and L. Streit (Eds.), *Stochastic Processes in Physics and Engineering*, Reidel Publishing Company, Dordrecht, 1988.

C. Jones and H. F. Jelinek Wavelet Packet Fractal Analysis of Neuronal Morphology, *Meth. Enzymology* 24(4), 2001.

M.A. Mainster, The fractal properties of retinal vessels: embryological and clinical implications. *Eye*, 4:235-241, 1990.

O. Rioul and M. Vetterli, Wavelets and signal processing, *IEEE Signal Processing Magazine*, 14-89, 1991.

T.Spencer, J. A. Olson, K.C. McHardy, P. F. Sharp, J. V. Forrester, An Image-Processing Strategy for the Segmentation and the Quantification of Microaneurysm in Fluorescein Angiograms of the Ocular Fundus, *Computers and Biomedical Research*, 29, 284-302, 1996.

E.J. Susman, W.J. Tsiaras, K.A. Soper, Diagnosis of diabetic eye disease, *JAMA*, 247:3231-3234, 1982.

T.Walter, J.C.Klein, P. Massin, F. Zana, Automatic Segmentation and Registration of Retinal Fluorescein Angiographies, *Proc. International Workshop on Computer Assisted Fundus Image Analysis* (Herlev Hospital, Copenhagen, Denmark, November), 2000.